Strathprints Institutional Repository

Norris, G and McConnell, G (2010) *Relaxed damage threshold intensity conditions and nonlinear increase in the conversion efficiency of an optical parametric oscillator using a bi-directional pump geometry.* Optics Express, 18 (5). pp. 3993-3999. ISSN 1094-4087

Relaxed damage threshold intensity conditions and nonlinear increase in the conversion efficiency of an optical parametric oscillator using a bi-directional pump geometry

G. Norris* & G. McConnell

Centre for Biophotonics, SIPBS, University of Strathclyde, 27 Taylor Street, Glasgow, G4 0NR, United Kingdom
**Corresponding author email: greg.norris@strath.ac.uk*

Abstract: A novel bi-directional pump geometry that nonlinearly increases the nonlinear optical conversion efficiency of a synchronously pumped optical parametric oscillator (OPO) is reported. This bi-directional pumping method synchronizes the circulating signal pulse with two counter-propagating pump pulses within a linear OPO resonator. Through this pump scheme, an increase in nonlinear optical conversion efficiency of 22 % was achieved at the signal wavelength, corresponding to a 95 % overall increase in average power. Given an almost unchanged measured pulse duration of 260 fs under optimal performance conditions, this related to a signal wavelength peak power output of 18.8 kW, compared with 10 kW using the traditional single-pass geometry. In this study, a total effective peak intensity pump-field of 7.11 GW/cm^2 (corresponding to 3.55 GW/cm^2 from each pump beam) was applied to a 3 mm long periodically poled lithium niobate crystal, which had a damage threshold intensity of 4 GW/cm^2, without impairing crystal integrity. We therefore prove the application of this novel pump geometry provides opportunities for power-scaling of synchronously pumped OPO systems together with enhanced nonlinear conversion efficiency through relaxed damage threshold intensity conditions.

OCIS codes: (190.4970) Parametric Oscillators and Amplifiers; (190.7110) Ultrafast Nonlinear Optics .

References and links

1. P J. A. Giordmaine & R. C. Smith, "Tunable coherent parametric oscillation in $LiNbO_3$ at optical frequencies", Phys. Rev., **14**, 24, (1965)
2. G. McConnell, "Nonlinear optical microscopy at wavelengths exceeding 1.4 µm using a synchronously pumped femtosecond-pulsed optical parametric oscillator", Phys. Med. Biol., **52,** 717-724, (2007)
3. B. J. Orr et al, "Laser spectroscopy with a pulsed, narrowband infrared optical parametric oscillator system: a practical, modular approach" J. Appl. Phys. B, **66**, 653 - 657, (1998)
4. J. A. Hutchinson et al, "Continuously tunable, 6-14 µm silver-gallium selenide optical parametric oscillator pumped at 1.57 µm", Appl. Phys. Lett.. **71** (5), 4, (1997)
5. E. Beaurepaire et al, "Imaging lipid bodies in cells and tissues using third-harmonic generation microscopy", Nat. Methods, **3**, 1, (2006)
6. H. Chen et al, "A multimodal platform for nonlinear optical microscopy and microspectroscopy", Opt. Express, **17**, 3, (2009)
7. M. H. Dunn & M. Ebrahimzadeh, "Parametric generation of tunable light from continuous-wave to femtosecond pulses", Science, **286**, 1513, (1999)
8. R. W. Boyd, "Nonlinear Optics", 2nd edition, (Academic Press), (2003), p99-106
9. Bjorkholm et al, "Improvement of optical parametric oscillators by nonresonant pump reflection", IEEE J. Quantum Electron, **6**, 12, (1970)
10. Yang et al, "Continuous-wave singly resonant optical parametric oscillator pumped by a resonantly doubled Nd:YAG laser", Opt. Lett., **18**, 12, (1992)
11. G. D. Boyd & A. Ashkin, "Theory of Parametric Oscillator Threshold with Single-Mode Optical Masers and Observation of Amplification in $LiNbO_3$", Phys. Rev., **146**, 187-199, (1966)
12. G. D. Boyd & D. A. Kleinman, "Parametric interaction of focused Gaussian light beams", J. Appl. Phys., **39**, 9, (1968)

1. Introduction

Since the first experimental demonstration of the optical parametric oscillator (OPO) by Giordmaine and Smith [1], advances in OPO technology have led to the realization of reliable, commercially available sources of coherent radiation. These sources have many applications including those in optical microscopy [2], spectroscopy [3], and also military purposes [4]. Such applications often capitalize upon the wavelength tuning properties of OPO systems, but efficient and turnkey high power ultra-short pulsed (>50 mW, <1 ps) synchronously pumped systems are increasingly sought-after for nonlinear optical imaging [2, 5] and spectroscopy [6]. However, there are several limitations to the routine and practical development of OPO platforms with high output power.

Many high-power ultra-short pulsed laser sources such as the multi-Watt fs-pulsed Ti:Sapphire laser and the fs-pulsed Yb:YAG source are now commercially available for synchronous pumping of OPO systems, but the nonlinear crystalline media employed usually have very low damage threshold intensities. Typically, the damage threshold intensity for nonlinear optical crystals employed in OPO systems is around a few GW/cm^2 [7]. Consequently, this restricts the total maximum pump intensity that can be applied.

Judicious design of the pump geometry has previously been shown to overcome this limitation to some extent. Most ultra-short pulsed singly resonant OPO systems employ a single-pass pump geometry but the conversion efficiency is low due to the short interaction lengths [8]. To increase the nonlinear optical conversion efficiency through increased interaction of light with the nonlinear crystal, double pass geometries have been employed. This includes the non-resonant reflection of the un-depleted pump beam after propagation through the nonlinear crystal either by reflection from an OPO cavity mirror [9] or a highly reflecting mirror external to the OPO resonator [10]. However, this double pass approach cannot easily be incorporated into synchronously pumped ultra-short pulsed OPO systems due to the requirement for temporal overlap of subsequent pump pulses, and high power operation remains difficult because of the low damage threshold intensity of the crystal.

We address this limitation by employing a novel bi-directional pump geometry for a singly resonant synchronously pumped ultra-short pulsed OPO. Instead of employing a conventional single-pass geometry, by simultaneously synchronizing a 'forward' pump pulse and a second counter-propagating pulse in the 'reverse' direction together with the circulating signal pulse, the signal electric field amplitude experiences gain in both directions and hence the resulting average output power scales nonlinearly with the overall input pump power. By ensuring only one pump pulse with an intensity level below the damage threshold intensity is present in the nonlinear crystal at any given time, this technique permits a total pump intensity of up to twice the damage threshold intensity, without incurring damage. As a consequence, the crystal damage threshold intensity conditions can be relaxed and the average and peak output powers of the OPO can be significantly increased

2. Theory

In order to describe the behavior of the pump (ω_1), signal (ω_2) and idler (ω_3) frequencies upon propagation through the nonlinear crystal within an OPO, the coupled amplitude wave equations must be considered [11]:

$$\frac{dE_1}{dz} = \frac{\sigma_1}{2}\sqrt{\frac{\mu}{\varepsilon_1}}E_1 - \frac{i\omega_1}{2}\sqrt{\frac{\mu}{\varepsilon_1}}dE_3E_2^* \exp[-i\Delta kz] \qquad (1)$$

$$\frac{dE_2}{dz} = \frac{\sigma_2}{2}\sqrt{\frac{\mu}{\varepsilon_2}}E_2 - \frac{i\omega_2}{2}\sqrt{\frac{\mu}{\varepsilon_2}}dE_3E_1^* \exp[-i\Delta kz] \qquad (2)$$

$$\frac{dE_3}{dz} = \frac{\sigma_3}{2}\sqrt{\frac{\mu}{\varepsilon_3}}E_3 - \frac{i\omega_3}{2}\sqrt{\frac{\mu}{\varepsilon_3}}dE_1E_2 \exp[-i\Delta kz] \qquad (3)$$

It is clear from equation (2) that the magnitude of the electric field $\mathbf{E_2}$ of the signal frequency is dependent upon the interaction between the pump and the generated idler frequencies. In the event that a pump pulse overlaps with a circulating signal pulse within the nonlinear crystal a difference frequency mixing process occurs, resulting in an increase in the idler amplitude $\mathbf{E_3}$. This increased idler amplitude is then subject to mixing with the pump frequency over the length of the crystal *z*. Thus, amplification of signal pulses occurs upon passing through the crystal in the direction of propagation of the pump pulse.

This description is the basis for the signal amplification experienced in a conventional single-pass synchronously pumped OPO. However, where a linear OPO cavity is applied, a second pump beam may be introduced to the crystal in a direction counter-propagating to the original pump source. This can be explained by further analysis of equations (1-3). With the introduction of a reverse pump beam into the system, interaction between this additional pump field $\mathbf{E_1}$ with the circulation signal field $\mathbf{E_2}$ results in a difference frequency mixing process, producing an additional idler field $\mathbf{E_3}$. This increase in idler electric field in turn stimulates further generation of the signal field $\mathbf{E_2}$. As a result, the signal pulses experience parametric amplification in both directions upon propagation through the crystal, but only when both pump pulses are temporally and spatially synchronized with the circulating intracavity signal frequency pulse. This 'bi-directional' pumping geometry forms the basis for our study.

3. Experiment

Figure 1 shows the experimental geometry for bi-directional pumping. A continuous wave mode-locked Yb-doped fiber laser, with an average power of 2W and repetition rate of 80 MHz, (Fianium, Femtopower 1060-2-s) was used as the pump source and provided pulses of 280 fs duration at 1064 nm with a spectral width of 12 nm (FWHM). This TEM_{00} single-mode laser was propagated through a Faraday isolator (E2), providing 30 dB of isolation to prevent feedback into the pump oscillator. By fully blocking the pump beam between element 4 and 13, we refer to the direction of pumping as the 'forward' direction, or by blocking the pump between elements 4 and 5, it is referred to as the 'reverse' direction, as shown in Figure 1. In order to keep the peak intensity of the pump source below the damage threshold intensity of the nonlinear crystal, only 50% of the average intensity from the pump was used in a single-pass in either direction. By using a 50/50 thin-plate beam-splitter (E4), 1W of average power was therefore provided in both the forward and reverse pumping directions.

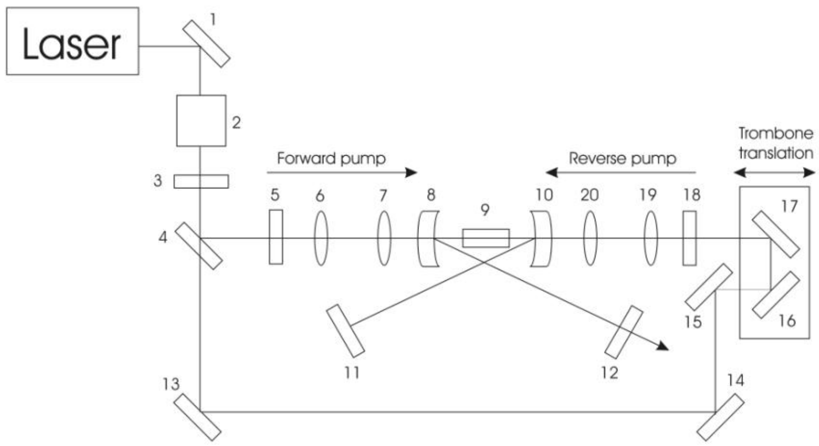

Fig. 1. Bi-directional pumped singly resonant OPO system. Element 1, 13, 14, 15, 16 and 17: highly reflecting at a wavelength of 1.064 µm. E2: faraday isolator. E3, 5 and 18: half wave plates. E4: beam-splitter (50/50 at the pump wavelength). E6, 7, 19 and 20: mode-matching optics. E8. 10, 11 and 12: cavity mirrors and E9: periodically poled lithium niobate crystal.

The polarizations of both beams were independently controlled by half-wave plates (E5, 18) designed for use at the pump wavelength. Both pump beams were then mode-matched to the linear OPO cavity using two sets of anti-reflection coated spherical lenses (E6, 7, 19, 20). The lenses were used to provide a pump beam radius of 20 µm in both the forward and reverse direction, which was determined by consideration of the Boyd-Kleinman focusing criterion [12]. To ensure a good temporal overlap for the reverse pump pulse and the circulating signal pulse, mirrors 16 and 17 were placed on a single translation stage creating a trombone arrangement to permit temporal displacement of the pump pulse in the reverse direction relative to the circulating signal wavelength pulse. Additionally, mirror 12 was placed on a translation stage to control synchronization of resonating pulses. A 3 mm long periodically poled lithium niobate (PPLN) crystal (E9) was designed to provide maximum output power at an OPO signal wavelength of 1500 nm. All of the mirrors in the OPO resonator were designed to be highly reflective at the signal wavelength and highly transmitting at pump and idler with the exception of the output coupler (E12), which was 50% reflecting at the signal wavelength. Additionally, elements 8 and 10 were zero lens mirrors with a ROC = 100 mm, with the cavity designed to provide a spot size of 19 µm at the focal point from both pump beams independently. The PPLN damage threshold intensity was experimentally demonstrated to be 4 GW/cm^2, which, when considering the pump source described previously, corresponded to a maximum single-pass pump average power of 1.1 W and a peak power of 49 kW. The PPLN crystal was anti-reflection coated at the pump wavelength on one surface only, namely the surface closest to the element 8, due to the crystal being a section cut from a longer PPLN crystal for this study. Neither surface was anti-reflection coated at the signal or idler wavelengths. This resulted in a substantial optical loss and which was therefore detrimental to the overall conversion efficiency. The crystal was kept in a home-made oven at a temperature of 100 ºC to ensure fixed signal wavelength operation.

4. Experimental results

Figure 2 shows the measured average signal output powers resulting from single-pass pumping in the forward and reverse directions independently. Also shown is the nonlinear increase in average power when both the forward and reverse pump pulses were synchronized with the resonating signal pulse, as per the bi-directional pump geometry described previously. The average powers obtained from the independent forward and reverse pumping schemes were 200 mW and 120 mW respectively, which in turn equated to pump depletions of 64 % and 47 %. This discrepancy in average output power, despite the similar characteristics of the pump pulses, arose as a result of the presence of the anti-reflection coating on only one surface of the crystal. The x-axis in Figure 2 represents the translation of the trombone stage (elements 16 and 17) which resulted in a synchronization of the reverse pump pulse and the resonating signal pulse created by the initial forward pump pulse.

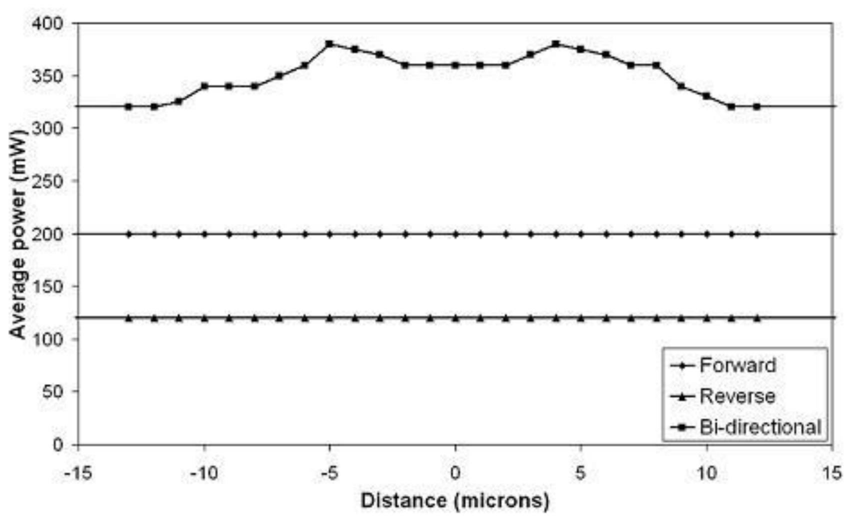

Fig. 2. Nonlinear increase in net average output power when forward and backward pump pulses were brought into synchronization with the resonating signal pulse. The x-axis zero point corresponds to exact overlap of the reverse pump and signal wavelength pulses.

As a result of applying an appropriate time-delay to the reverse pump pulse relative to the circulating signal wavelength pulse, an increase in average signal wavelength output power was achieved. In this demonstration, using the bi-directional pump geometry the average output power was measured to be 390 mW when the pump pulses were synchronized with the intracavity circulating signal wavelength pulse. This increase arises from the linear summation (120 mW + 200 mW) of the independent pump sources and a nonlinear increase of 22 % (70 mW) in average power when both pump pulses operate synchronously.

All average powers were measured using a calibrated calorimeter (Spectra-Physics, 407A) after transmission through a long-wave pass optical interference filter which was measured to be 85% transmitting at the signal wavelength (Thorlabs, FEL0450). Importantly, the generated output power was therefore higher than the measured 390 mW with an average output power of 460 mW (140 mW + 235 mW), corresponding to a net average power increase of 95 % observed at the signal wavelength when compared to the single-pass pumping in the forward direction.

Figure 3 shows the cavity length detuning tolerance when applying the forward, reverse and bi-directional pump geometries. Using the single-pass geometry in the forward direction, the maximum OPO cavity length detuning tolerance was 20 µm, which was approximately double that of the reverse pump geometry due to the optical loss previously described. When applying the bi-directional pump geometry, the OPO cavity length detuning tolerance increased to 40 µm. This indicated that the application of two separate pump beams partially compensated for the poor temporal synchronization of the pump/signal pulses while increasing the average output power at the signal wavelength.

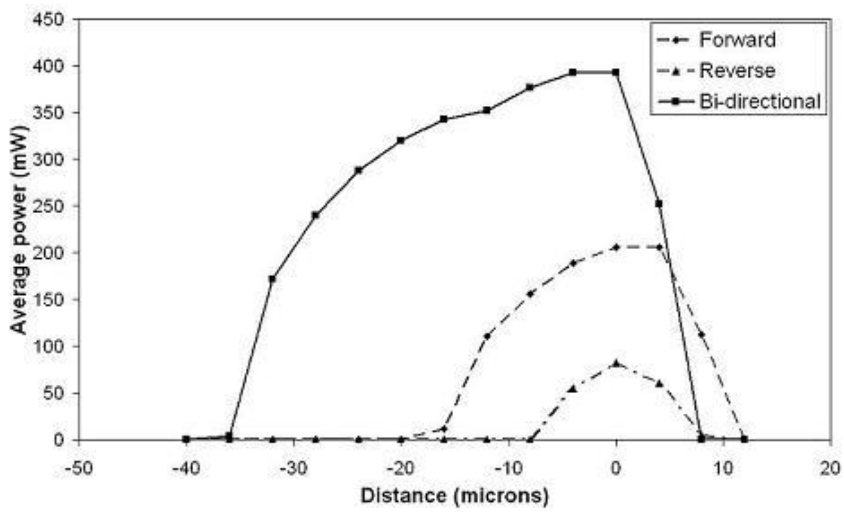

Fig. 3. Average output power at the signal wavelength as a function of cavity length detuning tolerance for the forward, reverse and bi-directional pumping schemes.

Pump pulse durations were measured in the forward and reverse directions (i.e. between elements 8 and 9 for the forward pump direction and between elements 9 and 10 for the reverse pump direction in Figure 1) and provided values of 280 fs in both directions.

Based on a sech-squared pulse shape, the resultant OPO signal wavelength pulses produced by the forward pump direction only were measured to be 250 fs in duration. However, for pumping in the reverse direction only, a pulse duration of 160 fs was measured. This variation was a result of imperfect pulse overlap experienced when aligning the OPO in the reverse direction while being required to maintain a constant the resonator length. When both forward and reverse pumping were synchronized as per the bi-directional pump geometry, a pulse duration of 260 fs was measured.

Figure 4 shows the effect on the OPO signal wavelength pulse duration upon detuning of the OPO cavity length. It was found that OPO signal wavelength pulse broadened from an optimal overlap value of 260 fs to a maximum pulse duration of 390 fs when approaching the edge of the OPO cavity length tuning range. Due to the 4 GW/cm^2 damage threshold intensity of PPLN, the pump pulse intensity had to remain below this value when applying the traditional single-pass pump geometry. However, applying the two separate pump beams as per the bi-directional pump geometry in synchronization with the circulating signal wavelength pulse, 2 W of overall average pump power could be applied to the crystal (1 W from each direction) without causing crystal damage. With the spot size within the PPLN crystal of around 20 µm, this corresponded to a total effective peak intensity of 7.11 GW/cm^2, which exceeded the damage threshold intensity of the material. By ensuring that only one pulse of intensity 3.55 GW/cm^2 was present in the crystal at any time, the damage intensity conditions were relaxed, permitting the application of total pump intensity at double that of the single-pass pump.

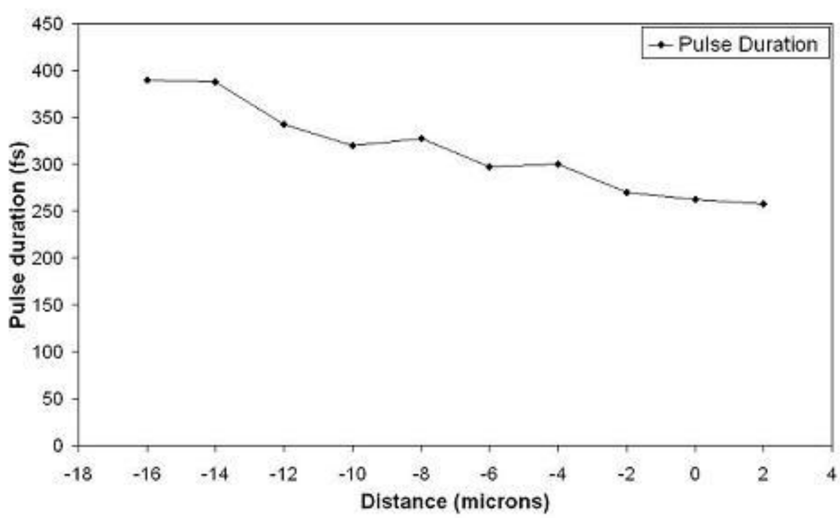

Fig. 4. Pulse duration of the signal wavelength output upon detuning the OPO cavity length.

5. Conclusion

In conclusion, this novel bi-directional pump geometry has been shown to relax the damage threshold intensity condition for nonlinear optical materials, thus enabling the application of higher power pump sources for singly resonant ultra-short pulsed OPO systems with a linear cavity. With a PPLN based singly resonant synchronously pumped OPO, at the OPO signal wavelength of 1500nm we measured an average output power of 390 mW using the bi-directional pump geometry, compared to a maximum of 200 mW when using the single-pass geometry. This increase arises from the linear summation (120 mW + 200 mW) of the independent pump sources and the nonlinear increase of 22 % (70 mW) in average power when two counter-propagating independent pump beams of 1 W average power were synchronized with the circulating signal wavelength pulse. By ensuring that only one pump pulse with 3.55 GW/cm^2 peak intensity was present in the PPLN crystal at any given time it was possible to pump the PPLN crystal at almost twice the intensity of the damage threshold intensity limit of PPLN. This technique also substantially increased the cavity length detuning tolerance of the resonator from a maximum of 20 µm to 40 µm, with less than a 50% variation in pulse duration across the cavity length detuning range.

This study was performed at fixed temperature (100 ºC) and we employed only one crystal period poling length for fixed wavelength operation of the OPO. However, given the multi-period structure within many commercially available PPLN crystals, wavelength tuning of the signal wavelength over a few hundreds of nanometers is possible through either temperature tuning of the crystal or by interaction of the pump beam with different period lengths. The described bi-directional pump geometry is theoretically compatible with both temperature tuning and with the application of alternative period lengths. Some adjustment of the temporal overlap of the reverse direction pump pulse relative to the circulating signal pulse through the trombone arrangement (E16 and E17 shown in Fig. 1) may be required to offset the change in temporal dispersion caused by the shift in signal wavelength. This will be investigated as part of a future study.

Acknowledgements

The authors would like to thank Research Councils UK and Coherent Ltd. for their financial support for this study.